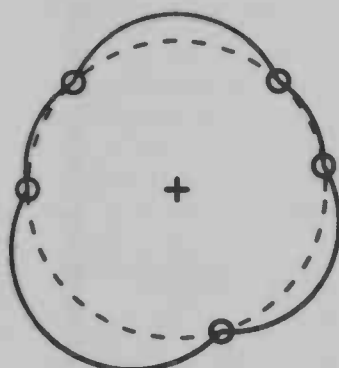


Master's Thesis

Certified reconstruction of convex curves using
radial basis functions



André Prins

*Institute for Mathematics and Computing Science
University of Groningen
The Netherlands*

Supervisor: Gert Vegter

23rd December 2004

The reconstruction of a curve or surface from an unorganized set of points is a well known problem. It is important in image analysis, but also in computer-aided design and the reverse engineering of surfaces. One of the methods for solving the surface reconstruction problem uses radial basis functions to construct an implicit surface interpolating each point of the input set. There are, however, no theoretical guarantees concerning the topological correctness of such an approximation.

This master's thesis deals with the reconstruction of convex curves in the plane using radial basis functions. In this case, an implicit curve is constructed as the collection of points where a function evaluates to zero. The function is constructed as a linear combination of radial basis functions centered at the input points. A linear system results from the requirement that each input point belongs to the curve. Using the solution to the linear system the function is found and the curve can be reconstructed from the set of points where the function evaluates to zero.

For samplings of a circle and the identity as the radial basis function, it is proven that the reconstruction is a topologically correct approximation of a circle. The same result is achieved for general convex curves under a general condition on the coefficients of the linear system.

Contents

1	Introduction	3
1.1	Research goals	3
1.2	Report overview	4
2	Related Work	5
2.1	Least squares planes	5
2.2	Delaunay based	6
2.2.1	Definitions	6
2.2.2	The crust	7
2.2.3	The algorithm:	7
2.2.4	Summary	8
2.3	Convex combinations	8
2.3.1	Reconstruction	8
2.3.2	Curve reconstruction	9
2.4	Modelling with radial basis functions	10
2.4.1	Inside constraints	11
2.4.2	Outside constraints	11
2.4.3	Normal constraints	11
2.4.4	Summary	12
3	Mathematical Background	13
3.1	Implicit surfaces	13
3.1.1	Advantages and disadvantages of implicit surfaces	14
3.2	Radial basis interpolation	14
3.3	Example: Thin-plate	15
4	Problem Definition	17
4.1	Topological correctness	17
4.2	Initial conjecture	19
4.3	Need for a condition on the sampling density	20
5	Main Result	21
5.1	Determining the interpolant	22
5.1.1	The value of the weights	23
5.1.2	Determination of the first N weights w_i	25
5.1.3	Determination of the additional weight w_+	25
5.1.4	Proof of Theorem 5.1	25
5.2	Gradient never perpendicular to a line	26

5.2.1	Proof for the negative projection	27
5.3	The function becomes negative	28
5.4	Proof of isotopy	28
5.5	Corollary: Curve lies outside the circle	29
5.5.1	Proof for the curve outside the circle	29
5.6	Generalization to convex curves	31
5.6.1	F is monotonically decreasing	31
5.6.2	The function becomes negative	32
5.6.3	Conclusion	32
6	Conclusion	33
6.1	Future work	33
A	Trigonometric Identities	36
A.1	Weight simplification	36
A.2	Tan sin to cos	36
A.3	Sum reduction	37
A.4	Proof for the inverse of the distance matrix	38

Chapter 1

Introduction

The problem of reconstructing a curve or surface from an unorganized set of points is well known in Computer Graphics and Computational Geometry. It is, for example, used in image analysis to reconstruct edges from a set of pixels possibly belonging to the edges. Another important area is the modelling or reverse engineering of surfaces. With reverse engineering, a 3D laser scan of a manufactured or natural (e.g. skull) object is created. A digital representation of the object must be created from this laser scan for further processing. Another option is to model an object directly using a free-form tool, where the modeller specifies points belonging to the surface and the free-form tool must construct a surface interpolating the points.

In many of these cases the data is given as an unorganized cloud of points sampled from the boundary of some object. This can be a real object scanned by a laser scanner or the shape desired by the modeller. In either case, a suitable surface representation must be created from the point cloud, interpolating each point and preferably approximating the desired surface closely.

1.1 Research goals

The main task of the reconstruction algorithm is to **construct** a surface which interpolates the given cloud of points. It is also desirable if the resulting surface S' is in some way a good approximation of the original surface S from which the points were sampled. This can mean, for example, that the resulting surface must have the same topology and hence the same number of components, holes, etc. as the original surface. It can also mean that the error (e.g. the Hausdorff distance) between the original surface S and the reconstructed surface S' must be below a certain threshold.

Many approaches have been proposed for solving this problem. Some of these approaches even give theoretical guarantees: **The reconstructed surface has the same topology as the original surface.**

In this master's thesis the reconstruction method using radial basis functions is examined. While the method is already widely used and gives good results, there are, so far, no theoretical guarantees concerning the topological correctness of the reconstructed curve or surface, except that the curve or surface interpolates

the input set. Therefore, the goal of this master's research is to find conditions for which the reconstruction of a curve in the plane using radial basis functions (RBF-reconstruction) gives a correct approximation of the curve.

When using radial basis functions to reconstruct a curve from a set of points, these points are considered as constraints on an implicit function. To correctly specify the inside and the outside of the curve, some additional constraints are needed, which is explained in the last part of Chapter 2. How to place these additional constraints is the main research question:

Where should these additional constraints be placed such that the reconstruction using radial basis functions (RBF-reconstruction) of the input constraints derived from the input set and the additional constraints gives a topologically correct result?

1.2 Report overview

The remainder of the report has the following structure: In the next chapter some other work on surface reconstruction is presented, where all approaches try to compute a piecewise linear approximation of the surface. In the last part of Chapter 2 a method will be described where radial basis functions are used for the modelling and design of surfaces. In Chapter 3 some required mathematical background will be presented, including an explanation of radial basis functions. Chapter 4 will present a more formal problem definition. In Chapter 5 the main result of this master's thesis will be presented. The last chapter will summarize the results of the report and will show unfinished work and remaining research directions.

Chapter 2

Related Work

A lot of research has already been performed on the (re)construction of curves and surfaces from an unorganized set of points, especially in 2D and 3D. In the past a number of methods has been proposed for solving the surface reconstruction problem from an unorganized set of points P . Most of these methods try to create a piecewise linear approximation of the curve or surface. Three methods are discussed, which will be described in the following three sections.

Least squares planes: A signed distance function is created from least squares planes passing through neighborhoods of points. From this signed distance function a polygonal approximation of the surface is constructed.

Delaunay based: A Delaunay triangulation is constructed from a point set derived from P . The piecewise linear approximation of the surface is extracted from this Delaunay triangulation.

Convex combinations: The input set P is mapped into a point set P^* in the plane, after which a normal triangulation method can be used on the points in the plane. A piecewise linear approximation of the surface is computed by mapping the triangulation in the plane back to 3D.

2.1 Least squares planes

The first method for surface reconstruction from an unorganized set of points is proposed by Hoppe *et al.* [11]. His method consists of two stages:

1. A function $f : \mathbb{R}^3 \rightarrow \mathbb{R}$ is defined, such that f is an estimation of the distance to the unknown surface.
2. A polygonization of the zero-set of f is created, which results in a piecewise linear approximation of the unknown surface.

The distance to the unknown surface is estimated by creating tangent planes as local approximations to the surface. A tangent plane is associated with each input point p_i as the plane through a neighborhood of, say k points, such that it is the best (least squares) approximation of a plane through all the points in the neighborhood. The estimated distance to the surface $f(x)$ of an arbitrary

point x to the surface is then the distance to the tangent plane with its center point (one of the input points p_i) closest to x .

The sign of the distance is determined by the orientation of the tangent plane and the position of x with respect to the tangent plane. To correctly compute the sign of the distance $f(x)$ it is necessary that the orientation of the tangent planes is consistent. When given two data points p_i and p_j close to each other, their corresponding tangent planes have normals n_i and n_j . These two normals must have roughly the same direction. This implies that for these two tangent planes: $\langle n_i, n_j \rangle \approx 1$.

A normal n_j with a small angle between n_i and n_j is preferred over propagating to a normal n_k with a large angle between n_i and n_k , while Propagating the orientation of n_i . By doing so it is ensured that the propagation is performed correctly.

A variation of the Marching Cubes algorithm [12] is used for the polygonization of the zero-set of the estimated distance function f .

2.2 Delaunay based

The first methods for topologically correct curve or surface reconstruction originate from the field of Computational Geometry and several theoretical guarantees were produced concerning the correct reconstruction of a curve or surface. Amenta *et al.* [2] gave the first provably correct algorithm, which produces a piecewise linear curve from an unorganized set of points in the plane.

2.2.1 Definitions

The proof involves the notion of an ϵ -sample and some definitions about the medial axis of the curve:

DEFINITION 2.1

The medial axis $MA(C)$ of a curve C is the closure of all points inside C with two or more closest points on C .

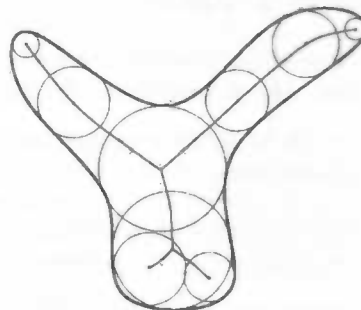


Figure 2.1: Example of the medial axis of a curve. The circles centered on the medial axis are medial balls.

The medial axis can be viewed as the collection of the centers of all maximal balls (medial balls) empty of points on C , but with two or more points of C on the balls boundary. An example of the medial axis is shown in Figure 2.1.

DEFINITION 2.2

The local feature size $LFS(p)$ of a point p is the distance of a point p to the medial axis.

This minimal distance is not necessarily the distance to the center of the medial ball which has p on its boundary.

A collection of points P is called an ϵ -sample if it satisfies the following condition:

DEFINITION 2.3

For each point $p \in C$ a point $q \in P$ with $\|p - q\| < \epsilon \cdot LFS(p)$ is sampled.

2.2.2 The crust

When decomposing the plane into Voronoi regions, the result is a collection of cells, with one cell $Vor(p)$ for each point p . The cell $Vor(p)$ is the set of all points in the plane closer to p than to any other point of the input set P . The collection of all these cells is called the Voronoi Diagram $\mathcal{V}(P)$ of P .

Using the definitions it is shown in [2] that each intersection $Vor(p) \cap C$ of a Voronoi cell with the curve must consist of one single curve segment containing the sample point p , if P is an ϵ -sampling with $\epsilon < 1$. This intersection is called the restricted Voronoi cell. When creating edges between each pair of points with adjacent restricted Voronoi cells a restricted Delaunay triangulation is created and this gives a representation of the adjacencies of the samples along the curve.

These adjacencies are represented by edges in the Delaunay triangulation and it is shown that for an ϵ -sample, with $\epsilon < 1$, this restricted Delaunay triangulation contains the required reconstruction and the reconstruction method must select exactly those parts which connect points which are adjacent on S .

2.2.3 The algorithm:

In the case of curve reconstruction a Voronoi diagram of the input set P is built. Let V denote the set of Voronoi vertices of this Voronoi diagram. It is sufficient to compute the restricted Delaunay triangulation by computing the Delaunay triangulation $\mathcal{D}(P \cup V)$, which is called the "raw crust". The correct reconstruction of the curve C can be computed as the union of those edges of $\mathcal{D}(P \cup V)$ with both endpoints in P and this results in the "crust".

The main theorem on curve reconstruction in [2] is:

THEOREM 2.1

For an ϵ -sample P of a curve C the crust of P is a topologically correct polygonal reconstruction of C , if $\epsilon \leq 0.252$.

A similar method is used for surface reconstruction, although direct filtering from $\mathcal{D}(P \cup V)$ is not sufficient. To construct the restricted Delaunay triangulation, poles are considered. A pole p^+ is defined as the vertex of a Voronoi cell $Vor(p)$ the farthest from the sample p and the pole p^- is defined as the vertex second farthest from the sample P . It is shown in [1] that the vector from p to p^+ is a nice approximation of the surface normal, which is used for filtering out triangle with too large a deviation between estimated and real triangle normal.

Let Q denote the union of all poles p^+ and p^- for each Voronoi cell $Vor(p)$. The restricted Delaunay triangulation is now constructed by creating the Delaunay triangulation of $P \cup Q$. The required triangles are filtered from $\mathcal{D}(P \cup Q)$ as those triangles with three samples as endpoints. Triangles with a large deviation between the triangle normal and the estimated surface normal are removed in a postprocessing step.

In [1] it is shown that this method results in a piecewise linear approximation of the surface S for an ϵ -sample with $\epsilon < 0.01$. In [3] this condition is improved to $\epsilon < 0.06$ and it is also shown that the distance between a point x and the reconstructed surface S is at most $\frac{1.15\epsilon}{1-\epsilon} LFS(x)$.

2.2.4 Summary

Based on the Delaunay triangulation of a set of points derived from the input set P , a correct reconstruction of the curve or surface is constructed if the input set P satisfies some conditions:

1. P is an ϵ -sample of the curve C with $\epsilon < 0.252$
2. For surface reconstruction, P is an ϵ -sample of the surface S with $\epsilon < 0.06$.

In several articles published by Dey *et al.* ([7], [6] and [3]) this algorithm is improved.

2.3 Convex combinations

A different method proposed by Floater in [10] for surface reconstruction is based on his method for parameterizing triangulations [9]. In his work on the parameterization of a triangulation the goal is to find a mapping which maps a piecewise linear surface patch (a triangulation \mathcal{T}) into a convex polygon in the plane, while preserving the adjacencies imposed by the triangulation \mathcal{T} .

As shown in [9] such a mapping can be found by using convex combinations: Demand that each vertex v from \mathcal{T} maps towards a vertex v^* in the plane, such that it is a convex combination of its neighbors in \mathcal{T} . Solving the resulting system allows for the construction of the mapping and in [9] it was proven that the resulting mapping is invertible if the boundary of \mathcal{T} is mapped into the boundary of a convex polygon in the plane.

2.3.1 Reconstruction

Within this framework, a convex combination mapping can be used for surface reconstruction: Given a collection of points p_i on a surface S , a piecewise linear

approximation must be found: A triangulation \mathcal{T} with exactly p_i as the set of vertices, which has the adjacency relations imposed by S .

In the case of creating a parameterization of a surface triangulation, a mapping must be found, mapping the entire surface patch into some convex region in the plane, which preserves the adjacency relations as imposed by \mathcal{T} . The problem of reconstructing a surface can be described as finding the adjacency relations.

This is done by first making a guess of the neighbors for each point: Collect around each point p_i a collection of K points p_j (e.g. use $K = 20$). This results in a graph with a large number of edges (candidate neighbors). Map these points using the candidate neighborhoods into the plane using a convex combination mapping $\varphi : \mathbb{R}^3 \rightarrow \mathbb{R}^2$. This method works only when the surface has a boundary and this boundary is known. In [10] this boundary is extracted manually from the input set, although an automatic method is also devised.

As is stated in [8] a convex combination mapping is always found if each point can be connected to a boundary point by following the guessed adjacencies. Intuitively, this implies that the set of candidate neighbors must not be too small.

The result of the mapping will be a collection of points p_i^* in a convex polygon in the plane. This can be triangulated using a standard triangulation method (e.g. Delaunay triangulation) resulting in a triangulation \mathcal{T}^* in the plane.

In [10] it was shown that the inverse φ^{-1} of the mapping φ exists. This inverse mapping is used to map the triangulation \mathcal{T}^* back into \mathbb{R}^3 . This results in the desired piecewise linear surface \mathcal{T} approximating the surface S .

2.3.2 Curve reconstruction

This method can also be used for the reconstruction of a curve in any number of dimensions. However, for this method a proof has been given in [8] concerning the correctness of the reconstruction.

When reconstructing a curve $C \subset \mathbb{R}^d$ between two endpoints x_0 and x_{n+1} from a given collection of points X , a mapping ($t : [0, 1] \rightarrow \mathbb{R}^d$) must be found mapping the straight line into the curve. The mapping can be found by computing a piecewise linear mapping using convex combinations which preserves the ordering of the points along the curve.

Around each point x_i a neighborhood N_i of points is collected. Each point $x_j \in N_i$ is within a ball of radius R_i centered at a point x_i . The parameters $t_i = t(x_i)$ are computed for each point using weights $\lambda_{i,j}$ between each pair of points x_i and x_j with each weight satisfying

$$\begin{aligned} \lambda_{i,j} &> 0 && \text{if } x_j \in N_i \\ \lambda_{i,j} &= 0 && \text{if } x_j \notin N_i. \end{aligned}$$

This results in the equation for each point x_i :

$$t(x_i) = t_i = \frac{1}{\sum \lambda_{i,j}} \sum_{j=0}^{n+1} \lambda_{i,j} t_j.$$

When rewriting this equation to

$$\sum_{j=1}^n -\lambda_{i,j}t_j + \sum_{j=0}^{n+1} \lambda_{i,j}t_j = \lambda_{i,0}t_0 + \lambda_{i,n+1}t_{n+1},$$

it can be written as $A \cdot \mathbf{t} = \mathbf{b}$ with

$$a_{ij} = -\lambda_{i,j}, \quad a_{ii} = \sum_{j=0}^{n+1} \lambda_{i,j}, \quad b_i = \lambda_{i,0}t_0 + \lambda_{i,n+1}t_{n+1}.$$

Solving for \mathbf{t} results in a collection of parameters t_i . When ordering the points x_i according to their parameter value t_i the curve can be reconstructed by creating edges between two points which are adjacent in the ordered sequence.

It was proven in [8] that this method gives a correct reconstruction of a curve under some conditions on the neighborhoods:

1. Each point x_i must be within the candidate neighborhood of its adjacent point x_{i+1} and vice versa: $x_i \in N_{i+1}$ and $x_{i+1} \in N_i$
2. Each point x_j must be closer to x_i than to x_{i+1} for $j < i$, while it must be closer to x_{i+1} than to x_i for $j > i$.

While a proof is given for correct curve reconstruction, there is no proof for the reconstruction of surfaces using this method. Nonetheless, useful results have been obtained with surface reconstruction using convex combinations.

2.4 Modelling with radial basis functions

A different area of research is concerned with the modelling of surfaces in computer-aided design. Several methods have already been proposed for the design of surfaces, but most of them use parametric surface patches. In [15] an approach is given for the modelling of implicit surfaces by specifying the points, which the desired surface must interpolate. The desired surface is then computed using a RBF-reconstruction method.

It is shown in [15] that it is necessary to distinguish the inside from the outside of the surface, which can be performed by specifying some additional constraints. Three methods were presented for distinguishing the inside from the outside of the surface:

1. Placing a few additional constraints on the inside.
2. Placing several additional constraints on the outside.
3. Placing constraints at specific points in the direction of the desired surface normal.

2.4.1 Inside constraints

The placement of a single constraint, which specifies the inside of the curve, is for several input sets sufficient to construct a single component interpolating each point. An example of this is shown in figure 2.2(a). The curve interpolates the collection of small circles, while only one additional point (the +) is specified inside the curve. As shown in figures 2.2(b) and 2.2(c) the exact position of the inside constraint influences the shape of the curve although it still remains a single component.

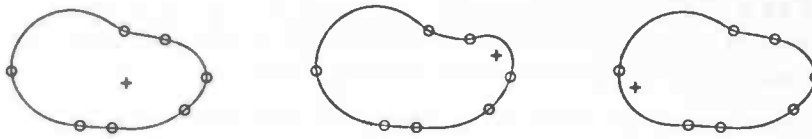


Figure 2.2: Demonstration of placing inside constraints.

2.4.2 Outside constraints

A method found to be especially useful for the design of curves was to place several constraints around the desired curve. This is shown in figures 2.3(a) and 2.3(b). In this case the number of components does not change when placing the additional constraints in a different way, while the shape is influenced by the placement of the additional constraints outside the curve.

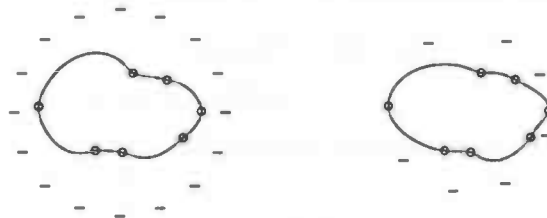


Figure 2.3: Demonstration of placing outside constraints.

2.4.3 Normal constraints

The last method proposed in [15] is to place additional constraints to specify the desired curve normal. Inside constraints and outside constraints are placed, such that they lie along the direction of the desired curve normal. In this way the modeller of the curve has a lot of control over the shape of the curve. This is demonstrated in figures 2.4(a), 2.4(b) and 2.4(c). The desired normal at one input point is changed in the middle figure and at two input points in the right figure.

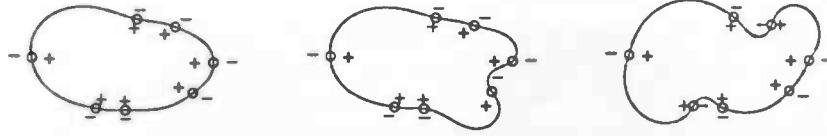


Figure 2.4: Demonstration of placing normal constraints.

2.4.4 Summary

As shown in the previous examples, the placement of additional constraints can have large effects on the shape of the resulting curve.

The remainder of the article shows how radial basis functions can be used to create implicit surfaces from polygonal models, which is not a research direction for this project.

Chapter 3

Mathematical Background

Before presenting the obtained results, some mathematical background will be given, including an explanation of radial basis functions.

Because the result of the reconstruction using radial basis functions is an implicit surface, a definition of implicit surfaces will be given in the first part of this chapter, together with some of their properties. The next part of the chapter will present the main theory for variational methods, which forms the basis for the reconstruction of a surface using radial basis functions. In the remaining parts of the chapter an example of a well-known problem will be given, which can be solved using radial basis functions.

3.1 Implicit surfaces

An implicit surface is the surface $S \subset \mathbb{R}^d$ derived from an implicit function $f : \mathbb{R}^d \rightarrow \mathbb{R}$ as

$$S = \{x \in \mathbb{R}^d \mid f(x) = 0\},$$

which is commonly denoted by $f^{-1}(0)$.

The surface S is called a regular surface whenever the gradient ∇f vanishes nowhere on the surface S .

$$\forall p \in S : \nabla f(p) \neq 0.$$

The sphere is a classical example of an implicit surface (Figure 3.1(a)). It is the collection of points with the same distance R to the center of the sphere. If the center of the sphere is at the origin then,

$$f(x, y, z) = x^2 + y^2 + z^2 - R^2.$$

Another example of an implicit surface is a torus (Figure 3.1(b)). If the torus is also centered at the origin then the implicit function is

$$f(x, y, z) = (x^2 + y^2 + z^2 + r_1^2 - r_2^2)^2 - 4r_1^2(x^2 + y^2),$$

with the additional condition that $r_1 > r_2$.



Figure 3.1: Two examples of implicit surfaces: A sphere on the left and a torus on the right.

3.1.1 Advantages and disadvantages of implicit surfaces

Implicit surfaces are very useful for the modelling of smooth deformable objects, which is not an easy task using polygonal models or parametric surface patches. Blending two implicit surfaces together is merely a matter of interpolation, while polygonal representations require sophisticated machinery for this blending process. Furthermore, implicit surfaces give a very general type of representation of surfaces, where many surfaces can be specified using combinations of simple functions. Finally, implicit surfaces are easy to ray-trace and can also be used in constructive solid geometry.

One of the biggest disadvantages of implicit surfaces is the fact that ray-tracing implicit surfaces can not be performed at interactive rates and that a polygonal model must be constructed in many cases.

3.2 Radial basis interpolation

The goal of the method is to reconstruct a surface from a given set of constraint points $P = \{p_1, \dots, p_N\} \subset \mathbb{R}^d$, which are to be interpolated by the desired surface. When viewing the desired surface as the zero-set of a function (f), the goal is to find a function $f : \mathbb{R}^d \rightarrow \mathbb{R}$ which satisfies the interpolation constraints $f(p_i) = 0$. Together with the criterion that the surface is a smooth surface, this can be viewed as a scattered data interpolation problem, where a function must be constructed satisfying the constraints $f(p_i) = h_i = 0$, while the smoothness is measured by an energy function which must be minimized.

To prevent a trivial solution ($f = 0$), some additional constraints on the function are required. This means that additional points must be placed where the function has a non-zero value. These additional constraints distinguish the inside from the outside of the surface. In Section 2.4 three methods for placing these constraints were explained.

This problem where a function must be found satisfying a collection of constraints while minimizing a certain energy function is called a scattered data interpolation problem and is a problem for which many numerical algorithms exist. But these algorithms discretize the region of interest, which automatically implies that the resolution is independent of the number of constraints.

It would sometimes be desirable if the accuracy of the approximating surface depends on the number of constraints, instead of on the discretization accuracy. Radial basis functions can be used on such an occasion. The desired function f is expressed as a linear combination of radial basis functions ϕ centered at the constraints:

$$f(x) = \sum_{i=1}^N w_i \phi(\|x - p_i\|) + Q(x) \quad (3.1)$$

In this expression $Q(x)$ denotes a linear polynomial which adds a linear and constant portion to f . In [14] it is shown that this polynomial is required to guarantee that the desired function f is a unique solution satisfying the interpolation constraints and the minimization constraint.

The constraints $f(p_j) = h_j$ imply

$$f(p_j) = \sum_{i=1}^N w_i \phi(\|p_j - p_i\|) + Q(p_j) = h_j.$$

When adding the additional constraints $\sum w_i = 0$ and $\sum w_i p_i = 0$ a linear system results:

$$\begin{pmatrix} D & p \\ p^T & 0 \end{pmatrix} \cdot \begin{pmatrix} w \\ q \end{pmatrix} = \begin{pmatrix} h \\ 0 \end{pmatrix}.$$

The part D in the matrix denotes the submatrix filled with elements related to the distances between the constraint points: $D_{ij} = \phi(\|p_i - p_j\|)$. The part q denotes the coefficients of the linear polynomial Q and p corresponds to the matrix filled with the coordinates of each point p_i . They are required for the evaluation of the polynomial.

When assuming that the linear system is non-singular, it can be solved and the resulting weights can be used to construct the desired function f , which satisfies all constraints. The resulting surface can be extracted using a polygonization method, e.g. the ones proposed by Boissonnat *et al.* [4], Boissonnat and Oudot [5] or Plantinga and Vegter [13].

The minimization of energy as mentioned in the beginning can be achieved by choosing a specific radial basis function ϕ . An example of this will be shown in the next section.

3.3 Example: Thin-plate

A well-known example of scattered data interpolation is **thin-plate** interpolation. In this specific situation the input is a set of points p_i in the plane with their desired heights h_i . From these constraints the goal is to construct a “smooth” function $f : \mathbb{R}^2 \rightarrow \mathbb{R}$, interpolating the constraints. The smoothness criterion is expressed by an energy-function $E(f)$:

$$E(f) = \int_{\Omega} f_{xx}^2(v) + 2f_{xy}^2(v) + f_{yy}^2(v) dv$$

In this expression the second partial derivative of f with respect to x is denoted by f_{xx} . The curvature of the entire function over the region Ω is measured by

this energy-function and is a means of measuring the curvature of the desired height field. The curvature must be minimized to produce satisfactory results and it can be proven [14] that choosing $\phi(r) = r^2 \log r$ as the radial basis function satisfies the minimization condition.

This approach is very similar to the process of placing a (very thin) plate of metal over a set of different sized spikes. The resistance of the metal to bending ensures that the plate smoothly changes its heights, while simultaneously touching the tip of each spike.

Chapter 4

Problem Definition

The goal of this master's thesis is to find conditions for which the reconstruction using radial basis functions of a convex curve gives a topologically correct approximation. Because there are no known theoretical guarantees for correct RBF-reconstruction the research is initially performed in 2D and not for general dimensionality.

As shown previously in Section 2.4, the placement of additional interior and exterior constraints greatly influences the shape and topology of the resulting curve. This is also the main research direction: How should the additional constraints (exterior and interior) be placed, such that the reconstructed curve is guaranteed to be correct.

To further simplify the research, the most simple radial basis function is used: $\phi(r) = r$ and the polynomial is initially stripped from the constructed implicit function. When given an input set P the goal remains to determine the positions of the interior constraints P_+ and the exterior constraints P_- .

PROBLEM 4.1

How should the set of additional constraints P_+ and P_- be positioned such that the reconstructed curve, as the zero-set of the implicit function

$$F(x) = \sum_{p_i \in P} w_i \cdot \|x - p_i\| + \sum_{p_j \in P_+} w_j \cdot \|x - p_j\| + \sum_{p_k \in P_-} w_k \cdot \|x - p_k\|,$$

is guaranteed to be a topologically correct approximation of the original convex curve C from which P is sampled.

P, P_+ and P_- must be disjoint, such that $F(p) = 0$, for $p \in P$, $F(p) > 0$, for $p \in P_+$ and $F(p) < 0$, for $p \in P_-$.

4.1 Topological correctness

It only remains to determine a good notion of correctness. Intuitively, the reconstructed curve $S = F^{-1}(0)$ should have at least a shape "similar" to that of the original curve C . What this means formally is hard to explain, but one can argue that the curve S must have at least the same topology as C

(the same number of components). When a sampling of an ellipsoid results in a reconstruction consisting of two small circles, the reconstruction will be incorrect. An example of such a reconstruction is shown in Figure 4.1.



Figure 4.1: An example showing how S is not a correct reconstruction of C , because the number of components is not the same.

Furthermore, the desire will be that the distance between the original and the reconstructed curve is as small as possible. This can for example be expressed by using a Hausdorff distance.

DEFINITION 4.1

The Hausdorff distance $\mathcal{H}(A, B)$ between two sets A and B is defined as

$$\mathcal{H}(A, B) = \min (h(A, B), h(B, A))$$

where

$$h(A, B) = \max_{a \in A} \left(\min_{b \in B} (\|b - a\|) \right)$$

This is however a difficult definition to work with, because it is hard to say when a distance measure is small enough and the Hausdorff distance is very difficult to compute in many cases. Therefore, another condition will be used: The topology between the reconstructed and the original curve must be the same and the order of the points along the initial curve C must be preserved in the reconstructed curve S . The formal definition will then be:

DEFINITION 4.2

The reconstructed curve $S = F^{-1}(0)$ is a correct reconstruction of the curve C if an isotopy between the two curves can be constructed and the ordering of the points P on S is the same as the ordering of P on C .

This means that an isotopy must exist, which leaves the constraint points fixed. From the formal definition of isotopy there must exist a continuous and invertible mapping by which S can be deformed into C and vice versa. Then, for each point $p \in S$ a unique corresponding point $q \in C$ must exist and vice versa. In figure 4.2 it is shown how the object on the left is not isotopic to the object on the right, because there is no deformation possible without breaking the outer component on the right.

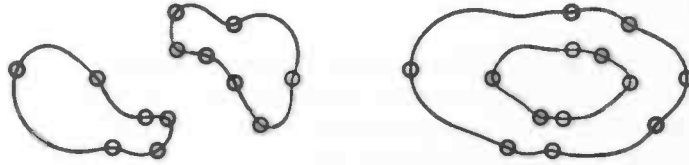


Figure 4.2: An example showing how S is not a correct reconstruction of C , because there is no deformation possible from the two components on the left to the two components on the right.

4.2 Initial conjecture

When experimenting with several input sets (samplings of a convex curve), it appears that the placement of a single interior constraint is sufficient to produce a correct reconstruction. This is the initial conjecture from which the research was started. In Figure 4.3 an example is given of two reconstructions of a convex polygon where the additional constraint is placed inside the polygon.



Figure 4.3: Two examples of the RBF-reconstruction from the vertices of a convex polygon. The function $\phi(r) = r$ is used as the radial basis function. A single additional constraint (the + in the figures) is used.

PROBLEM 4.2

When given the vertices $P = \{p_1, \dots, p_N\}$ of a convex polygon C in the plane, find out how the RBF-reconstruction from P as the zero-set of

$$F(x) = \sum_{i=1}^N w_i \cdot \|x - p_i\| + w_+ \cdot \|x - p_+\|$$

is guaranteed to be a topologically correct reconstruction of the original convex polygon C , where $F(p_i) = 0$ for each $p_i \in P$ and p_+ is placed inside C with $F(p_+) = 1$.

4.3 Need for a condition on the sampling density

The placement of a single constraint inside the convex polygon is often sufficient to guarantee a topologically correct reconstruction. For some collections of points the placement of a single constraint inside is not sufficient. An example of such an input set is shown in Figure 4.4

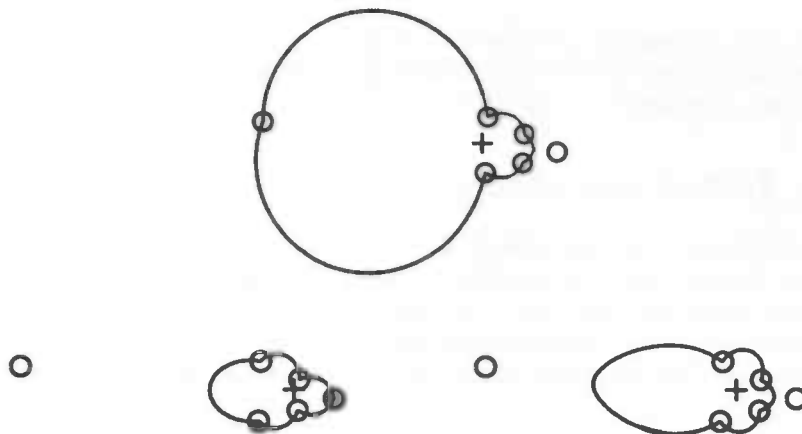


Figure 4.4: An example demonstrating that a single additional constraint inside is not always sufficient.

In the top figure an example is given of a reconstruction where the leftmost point is in the same component as the middle 4 points. The bottom left picture shows the reconstruction when moving the additional constraint to the right. Then the left point is not in the same component anymore, but the right point is. This means, intuitively, that moving the additional constraint a little to the left again could result in a component interpolating all the points. However, as is seen in the bottom right picture, this does not occur: Both the leftmost and the rightmost points are not in the same component as the middle point.

This is a good example of a point set where the reconstruction using only one additional constraint inside the convex polygon is insufficient for a topologically correct reconstruction. This implies also that some restrictions are required on the collection of input points. When considering the input set P as the vertices of a polygon C , the example in Figure 4.4 shows that the polygon has a sharp angle at the leftmost point. This must be prevented and for a theoretical guarantee it is probably required that the sampling of a convex curve is in some way dense enough.

Chapter 5

Main Result

The main result of this master's thesis concerns the topologically correct reconstruction of a specific version of a convex curve: A circle. The circle is a simple convex curve and is therefore chosen as the first type of convex curve to be examined. Hopefully, a proof for the topologically correct reconstruction of a circle can be extended easily towards a proof for general convex polygons.

Let P be a set of points $\{p_1, \dots, p_N\}$ in the plane lying on a circle C and with radius r . The point p_{i+1} is the successor of p_i , where the indices are cyclic.

Define an implicit function $F: \mathbb{R}^2 \rightarrow \mathbb{R}$ as

$$F(x) = \sum_{i=1}^N w_i \cdot \|x - p_i\| + w_+ \cdot \|x - p_+\| \quad (5.1)$$

and let this be constructed as the RBF-reconstruction which uses $\phi(r) = r$ as the radial basis function and with unknown weights w_i and w_+ . The points from the input set P are used as the zero-constraints on the function: $F(p_i) = 0$ for each $p_i \in P$ and p_+ is placed at the center of the circle where $F(p_+) = 1$. Let S be the zero-set of the function F , then the main result of this thesis is as follows:

THEOREM 5.1

If the angle between $\overrightarrow{p_i p_+}$ and $\overrightarrow{p_{i+1} p_+}$ is smaller than π for any two consecutive points p_i and p_{i+1} on the circle, then:

1. $S = F^{-1}(0)$ is isotopic to C .
2. The points p_i have the same order on S as on C .

The proof of this theorem is presented in the remainder of this chapter, where first an explicit expression for the function F is determined, followed by the proof of both parts of theorem 5.1.

5.1 Determining the interpolant

For simplicity, assume $p_1 = (r, 0)$. Notice that the set of points $P = \{p_1, \dots, p_N\}$ can be described by a set of angles:

$$A = \{\alpha_1, \dots, \alpha_N\} \quad \text{with } \alpha_i > 0 \quad \text{such that} \quad \sum_{k=1}^N \alpha_k = 2\pi,$$

such that, as demonstrated in Figure 5.1, each point p_i can be written as

$$p_i = \left(r \cos \sum_{k=1}^{i-1} \alpha_k, r \sin \sum_{k=1}^{i-1} \alpha_k \right).$$

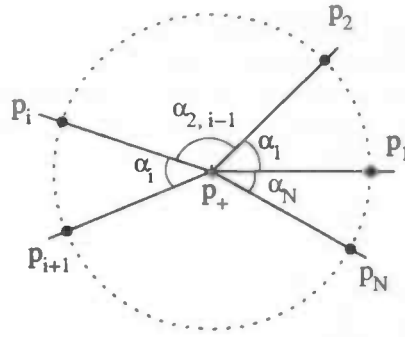


Figure 5.1: The angles determined by the set of points p_1, \dots, p_N and p_+ , where $\alpha_{2,i-1} = \alpha_2 + \dots + \alpha_{i-1}$.

Because of the specific distribution of the points p_i , the function F and its gradient ∇F can be derived from their positions:

LEMMA 5.1

$$F(x) = \frac{1}{2rT} \left[\sum_{i=1}^N \left(\tan \frac{\alpha_i}{4} + \tan \frac{\alpha_{i-1}}{4} \right) \cdot \|x - p_i\| - 4 \cdot \|x - p_+\| \right] \quad (5.2)$$

and

$$\nabla F(x) = \frac{1}{2rT} \left[\sum_{i=1}^N \left(\tan \frac{\alpha_i}{4} + \tan \frac{\alpha_{i-1}}{4} \right) \cdot \mathbf{v}_i(x) - 4 \cdot \mathbf{v}_+(x) \right]. \quad (5.3)$$

with

$$T = \sum_{i=1}^N \tan \frac{\alpha_i}{4}, \quad \mathbf{v}_j(x) = \frac{x - p_j}{\|x - p_j\|} \quad \text{and} \quad \mathbf{v}_+(x) = \frac{x - p_+}{\|x - p_+\|}$$

5.1.1 The value of the weights

For the proof of Lemma 5.1, the weights w_i and w_+ need to be determined.

LEMMA 5.2

$$w_i = \left(\tan \frac{\alpha_i}{4} + \tan \frac{\alpha_{i-1}}{4} \right) \cdot \frac{1}{2rT},$$

$$w_+ = -\frac{2}{rT} \quad \text{where} \quad T = \sum_{i=1}^N \tan \frac{\alpha_i}{4}.$$

Notice, for the proof of Lemma 5.2, that a set of equations results from the constraints for the points p_i and p_+ :

$$F(p_j) = 0 \quad \text{for } j = 1, \dots, N \quad \text{and} \quad F(p_+) = 1.$$

The constraints $F(p_j) = 0$ can be written as

$$\sum_{i=1}^N w_i \cdot \|p_j - p_i\| + w_+ \cdot \|p_j - p_+\| = 0, \quad \text{for } j = 1, \dots, N, \quad (5.4)$$

and $F(p_+) = 1$ can be written as

$$\sum_{i=1}^N w_i \cdot \|p_+ - p_i\| + w_+ \cdot \|p_+ - p_+\| = 1. \quad (5.5)$$

This is a set of $N + 1$ linear equations with $N + 1$ unknowns (the w 's).

Write

$$\varphi_{i,j} = \|p_i - p_j\| = 2r \sin \frac{1}{2} \sum_{k=i}^{j-1} \alpha_k \quad \text{and} \quad \varphi_{j,+} = \|p_j - p_+\| = r.$$

Hence $\varphi_{i,i} = \|p_i - p_i\| = 0$ and $\varphi_{i,j} = \|p_i - p_j\| = \|p_j - p_i\| = \varphi_{j,i}$. This allows the set of N equations derived from the zero-constraints (equation 5.4) to be written as

$$\sum_{i=1}^N w_i \varphi_{i,j} = -w_+ \varphi_{j,+} \quad \text{for } j = 1, \dots, N. \quad (5.6)$$

This can be viewed as a linear system: $\Phi \cdot \vec{w} = \vec{c}$ where

$$c_j = -w_+ \varphi_{j,+} = -w_+ r$$

For points in general position this matrix is non-singular and the system can be solved using a method like LU-decomposition, Gauss-elimination, etc.

Observe that the set of equations (equation (5.6)) can be written as

$$2r \cdot \Lambda \cdot \vec{w} = \vec{c},$$

where

$$\Lambda = \begin{pmatrix} 0 & \sin(\beta_1) & \dots & \sin(\beta_1 + \dots + \beta_{N-1}) \\ \sin(\beta_1) & 0 & \dots & \sin(\beta_2 + \dots + \beta_{N-1}) \\ \sin(\beta_1 + \beta_2) & \sin(\beta_2) & \dots & \sin(\beta_3 + \dots + \beta_{N-1}) \\ \vdots & \vdots & \ddots & \vdots \\ \sin(\beta_1 + \dots + \beta_{N-1}) & \sin(\beta_2 + \dots + \beta_{N-1}) & \dots & 0 \end{pmatrix},$$

with

$$\beta_i = \frac{\alpha_i}{2} \quad \text{and where} \quad \vec{w} = \begin{pmatrix} w_1 \\ \vdots \\ w_N \end{pmatrix} \quad \text{and} \quad \vec{c} = \begin{pmatrix} w + \varphi_{1,+} \\ \vdots \\ w + \varphi_{N,+} \end{pmatrix}$$

To solve this system the inverse of the matrix Λ is used. Consider now Lemma 5.3:

LEMMA 5.3 (INVERSE OF THE DISTANCE MATRIX)

Consider the matrix Λ filled with entries $\lambda_{i,j} = \sin \sum_{k=i}^{j-1} \beta_k$ for $1 \leq i \leq j \leq N$ and $\lambda_{j,i} = \lambda_{i,j}$ for $1 \leq j \leq i \leq N$.

$$\Lambda = \begin{pmatrix} 0 & \sin(\beta_1) & \dots & \sin(\beta_1 + \dots + \beta_{N-1}) \\ \sin(\beta_1) & 0 & \dots & \sin(\beta_2 + \dots + \beta_{N-1}) \\ \sin(\beta_1 + \beta_2) & \sin(\beta_2) & \dots & \sin(\beta_3 + \dots + \beta_{N-1}) \\ \vdots & \vdots & \ddots & \vdots \\ \sin(\beta_1 + \dots + \beta_{N-1}) & \sin(\beta_2 + \dots + \beta_{N-1}) & \dots & 0 \end{pmatrix}.$$

This matrix Λ is non-singular and the matrix Γ is its inverse: It is a banded matrix with a single band on both sides of the diagonal:

$$\Gamma = \begin{pmatrix} \mu_1 & \nu_1 & 0 & 0 & \dots & 0 & \nu_N \\ \nu_1 & \mu_2 & \nu_2 & 0 & \dots & 0 & 0 \\ 0 & \nu_2 & \mu_3 & \nu_3 & \dots & 0 & 0 \\ \vdots & \vdots & \vdots & \vdots & \ddots & \vdots & \vdots \\ \nu_N & 0 & 0 & 0 & \dots & \nu_{N-1} & \mu_N \end{pmatrix}.$$

The matrix Γ has entries $\gamma_{i,j} = 0$, except:

$$\begin{aligned} \gamma_{i,i} &= \mu_i = -\frac{1}{2} (\cot \beta_{i-1} + \cot \beta_i). \\ \gamma_{i,i-1} &= \nu_{i-1} = \frac{1}{2} \csc \beta_{i-1}. \\ \gamma_{i,i+1} &= \nu_i = \frac{1}{2} \csc \beta_i. \end{aligned}$$

Proof:

Lemma 5.3 is proven in Section A.4, because it involves expanding a lot of summations and using trigonometric identities and the proof itself is not really important for the remainder of this section.

5.1.2 Determination of the first N weights w_i

From the linear system $2r \cdot \Lambda \cdot \vec{w} = \vec{c}$ the vector \vec{w} can be determined as $\vec{w} = \frac{1}{2r} \cdot \Gamma \cdot \vec{c}$, resulting in the following expression for each w_i :

$$\begin{aligned} w_i &= -\frac{w_+ r}{2r} (\gamma_{i,i-1} + \gamma_{i,i} + \gamma_{i,i+1}) \\ &= -\frac{w_+}{4} \left(\csc \frac{\alpha_{i-1}}{2} + \csc \frac{\alpha_i}{2} - \cot \frac{\alpha_{i-1}}{2} - \cot \frac{\alpha_i}{2} \right). \end{aligned}$$

From Lemma A.1 each weight w_i can be written as

$$w_i = -\frac{w_+}{4} \left(\tan \frac{\alpha_{i-1}}{4} + \tan \frac{\alpha_i}{4} \right).$$

5.1.3 Determination of the additional weight w_+

From the expression for w_i the expression for w_+ can be derived by using equation (5.5) of the $+$ -constraint. Observe that:

$$\sum_{i=1}^N w_i \cdot \|p_+ - p_i\| + w_+ \cdot \|p_+ - p_+\| = 1 \quad \text{implies} \quad \sum_{i=1}^N w_i \cdot r = 1.$$

Filling in w_i results in

$$-\frac{w_+ r}{4} \sum_{i=1}^N \left(\tan \frac{\alpha_i}{4} + \tan \frac{\alpha_{i-1}}{4} \right) = 1.$$

Using

$$T = \sum_{i=1}^N \tan \frac{\alpha_i}{4} = \frac{1}{2} \sum_{i=1}^N \left(\tan \frac{\alpha_i}{4} + \tan \frac{\alpha_{i-1}}{4} \right),$$

yields

$$w_+ = -\frac{2}{rT}.$$

Now w_i can also be determined using w_+ :

$$w_i = \frac{2}{rT4} \left(\tan \frac{\alpha_i}{4} + \tan \frac{\alpha_{i-1}}{4} \right) = \frac{1}{2rT} \left(\tan \frac{\alpha_i}{4} + \tan \frac{\alpha_{i-1}}{4} \right)$$

and this concludes the proof for lemma 5.2 \square .

Notice that $T > 0$ for any collection of angles $\alpha_i > 0$, because $\tan \frac{\alpha_i}{4} > 0$ for $\alpha_i < 2\pi$. Another important property is the fact that all the weights w_i are positive. Using $\frac{\alpha}{4} < \tan \frac{\alpha}{4} < \frac{\alpha}{\pi}$ for $0 < \alpha < \pi$ allows T also to be bounded: $\frac{\pi}{2} < T < 2$.

5.1.4 Proof of Theorem 5.1

Now all the (previously unknown) weights have been determined. With these weights the RBF-interpolant F and its gradient ∇F can be found by substituting the expressions for each w_i and w_+ .

Function F

Filling in the known weights from Lemma 5.2 into the expression for RBF-interpolant from equation (5.1) results in

$$\begin{aligned} F(x) &= \sum_{i=1}^N \frac{1}{2rT} \left(\tan \frac{\alpha_i}{4} + \tan \frac{\alpha_{i-1}}{4} \right) \cdot \|x - p_i\| - \frac{2}{rT} \cdot \|x - p_+\| \\ &= \frac{1}{2rT} \left[\sum_{i=1}^N \left(\tan \frac{\alpha_i}{4} + \tan \frac{\alpha_{i-1}}{4} \right) \cdot \|x - p_i\| - 4 \cdot \|x - p_+\| \right], \end{aligned}$$

which proves equation (5.2) from Lemma 5.1.

Gradient ∇F

The gradient $\nabla F(x)$ of this function can also be derived:

$$\nabla F(x) = \sum_{i=1}^N w_i \cdot \nabla \|x - p_i\| + w_+ \cdot \nabla \|x - p_+\|.$$

Using

$$\nabla \|x - q\| = \frac{x - q}{\|x - q\|}$$

the gradient can be derived as

$$\nabla F(x) = \sum_{i=1}^N w_i \cdot \mathbf{v}_i(x) + w_+ \cdot \mathbf{v}_+(x),$$

where

$$\mathbf{v}_i(x) = \frac{x - p_i}{\|x - p_i\|} \quad \text{and} \quad \mathbf{v}_+(x) = \frac{x - p_+}{\|x - p_+\|}$$

Notice that ∇F is undefined at the constraint points p_i and at p_+ . Filling in the expressions for w_i and w_+ results in

$$\nabla F(x) = \frac{1}{2rT} \left[\sum_{i=1}^N \left(\tan \frac{\alpha_i}{4} + \tan \frac{\alpha_{i-1}}{4} \right) \cdot \mathbf{v}_i(x) - 4 \cdot \mathbf{v}_+(x) \right],$$

which proves equation (5.3) and completes the proof of Lemma 5.1.

5.2 Gradient never perpendicular to a line

To prove isotopy between S and C it is sufficient that each half-line \vec{l} directed outwards from p_+ intersects $S = F^{-1}(0)$ once. This can be accomplished by showing that along the half-line \vec{l} the function F is monotonically decreasing. It remains then to show that $F(q) < 0$ for any q with a large enough distance $\|q - p_+\|$ from p_+ .

LEMMA 5.4 (NEGATIVE PROJECTION)

If the angle between $\overrightarrow{p_i p_+}$ and $\overrightarrow{p_{i+1} p_+}$ is smaller than π for any two consecutive points p_i and p_{i+1} on the circle, then: The gradient of $F(q)$ for any point q outside or on the circle C has a negative projection on any half-line \vec{l} directed outwards from p_+ .

5.2.1 Proof for the negative projection

The gradient $\nabla F(q)$ lies along the direction of maximal increasing value of F at q . For most points this vector must then be directed approximately towards p_+ where $F(p_+) = 1$.

The line \vec{l} has direction $\mathbf{v}_+(q)$, so the projection of $\nabla F(q)$ on this line \vec{l} being negative is equivalent to

$$\langle \nabla F(q), \mathbf{v}_+(q) \rangle < 0. \quad (5.7)$$

Using bilinearity of the inner product, inequality (5.7) is rewritten as:

$$\frac{1}{2rT} \left[\sum_{i=1}^N \left(\tan \frac{\alpha_i}{4} + \tan \frac{\alpha_{i-1}}{4} \right) \cdot \langle \mathbf{v}_i(q), \mathbf{v}_+(q) \rangle - 4 \cdot \langle \mathbf{v}_+(q), \mathbf{v}_+(q) \rangle \right] < 0. \quad (5.8)$$

The facts that both r and T are positive and $\langle \mathbf{v}_+(q), \mathbf{v}_+(q) \rangle = \|\mathbf{v}_+\|^2 = 1$ imply that inequality (5.8) is equivalent to

$$\sum_{i=1}^N \left(\tan \frac{\alpha_i}{4} + \tan \frac{\alpha_{i-1}}{4} \right) \cdot \langle \mathbf{v}_i(q), \mathbf{v}_+(q) \rangle - 4 < 0.$$

Writing $\cos \beta_i = \langle \mathbf{v}_i(q), \mathbf{v}_+(q) \rangle$, this can be reduced to:

$$\sum_{i=1}^N \left(\tan \frac{\alpha_i}{4} + \tan \frac{\alpha_{i-1}}{4} \right) \cos \beta_i < 4. \quad (5.9)$$

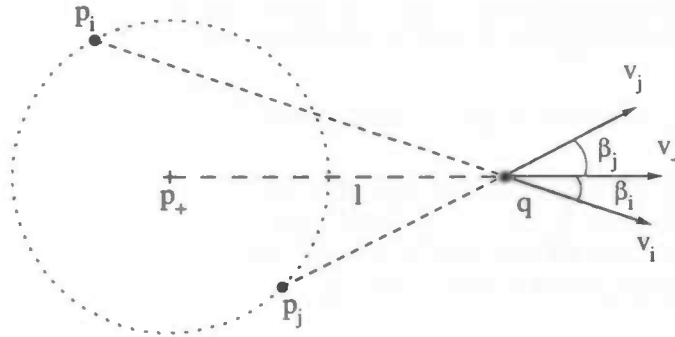


Figure 5.2: Demonstration of the vectors $\mathbf{v}_i(q)$ and $\mathbf{v}_+(q)$ and the angles β_i .

In Figure 5.2 the relation between the vectors \mathbf{v}_i and \mathbf{v}_+ and the angles β_i is shown. Since $0 \leq \cos \beta_i \leq 1$, for $i = 1, \dots, N$ and $\tan \frac{\alpha}{4} > 0$ for $0 \leq \alpha \leq 2\pi$:

$$\sum_{i=1}^N \left(\tan \frac{\alpha_i}{4} + \tan \frac{\alpha_{i-1}}{4} \right) \cos \beta_i < \sum_{i=1}^N \left(\tan \frac{\alpha_i}{4} + \tan \frac{\alpha_{i-1}}{4} \right).$$

Using $\tan \frac{\alpha}{4} < \frac{\alpha}{\pi}$ for $\alpha \in [0, \pi)$ yields

$$\sum_{i=1}^N \left(\tan \frac{\alpha_i}{4} + \tan \frac{\alpha_{i-1}}{4} \right) < \frac{2}{\pi} \sum_{i=1}^N \alpha_i = \frac{4\pi}{\pi} = 4.$$

In view of equation (5.9) this implies $\langle \nabla F(q), \vec{l} \rangle < 0$ when $0 < \alpha_i < \pi$ for each $i = 1, \dots, N$, completing the proof for Lemma 5.4 \square .

5.3 The function becomes negative

After proving that the function F is monotonically decreasing along any line directed outwards from p_+ (where $F(p_+) = 1$), it remains only to prove that the function becomes negative.

LEMMA 5.5

$$F(q) < 0, \quad \text{for any point } q \text{ with } \|q - p_+\| > \frac{T}{2-T} \cdot r$$

Consider the interpolant from equation (5.2) for any point q .

$$F(q) = \frac{1}{2rT} \left[\sum_{i=1}^N \left(\tan \frac{\alpha_i}{4} + \tan \frac{\alpha_{i-1}}{4} \right) \cdot \|q - p_i\| + w_+ \cdot \|q - p_+\| \right]$$

Consider now also the distance $\|q - p_i\|$ for any point q outside the circle: Then $\|q - p_i\| < \|q - p_+\| + r$. Let $G(q)$ be the function defined as

$$G(q) = \sum_{i=1}^N w_i \cdot (\|q - p_+\| + r) + w_+ \cdot \|q - p_+\|$$

For any point q outside the circle C it follows that $F(q) < G(q)$ and proving that $G(q) < 0$ also proves $F(q) < 0$. Reduce $G(q)$ to

$$G(q) = \frac{1}{2rT} [r \cdot 2T + \|q - p_+\| \cdot (-4 + 2T)]$$

Demanding that $\|q - p_+\| > \frac{T}{2-T} \cdot r$ satisfies $G(q) > 0$ and then also satisfies $F(q) > 0$. Because $\frac{\pi}{2} < T < 2$, the factor $\frac{T}{2-T}$ is always larger than 1 and it can be concluded that for any point q with $\|q - p_+\| > \frac{T}{2-T} \cdot r$ the function value $F(q)$ is negative, which proves Lemma 5.5.

5.4 Proof of isotopy

To prove isotopy between $S = F^{-1}(0)$ and C , it is required that a continuous invertible mapping exists between S and C , which deforms S into C .

Recall from Theorem 5.1 that each half-line \vec{l} directed outwards from p_+ intersects $S = F^{-1}(0)$ only once, just like the circle C . This holds when the angle between $\overrightarrow{p_i p_+}$ and $\overrightarrow{p_{i+1} p_+}$ is smaller than π for any two consecutive points p_i and p_{i+1} on the circle. From this an isotopy between the circle C and the RBF-reconstruction S is created, by linearly interpolating between each point q on S and the intersection point q' of the line directed outwards from p_+ and with direction $v_+(q)$. Because each point p_i is connected by an open segment of the curve S to the next point p_{i+1} , the ordering of the points P is also preserved, proving Theorem 5.1 for circles C centered at $(0,0)$ and with $p_1 = (r,0)$.

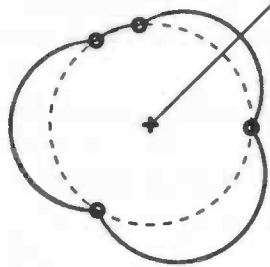


Figure 5.3: Construction of the isotopy, by projecting a point on S to its corresponding point on C and interpolating between them.

The weights are invariant to translation and rotation, because a translation or rotation does not change the distance matrix. Then F is also invariant to translation and rotation because it is a linear combination of distances. From this it follows that Theorem 5.1 holds for any circle with radius r .

5.5 Corollary: Curve lies outside the circle

Experiments with various point sets show that the resulting curve lies outside the circle in many cases. This can also be proven as the following lemma.

LEMMA 5.6 (OUTSIDE CIRCLE)

The function value $F(q)$ on any point q on the circle C is at least 0.

5.5.1 Proof for the curve outside the circle

Let q be a point on the arc of the circle C between p_N and p_1 .

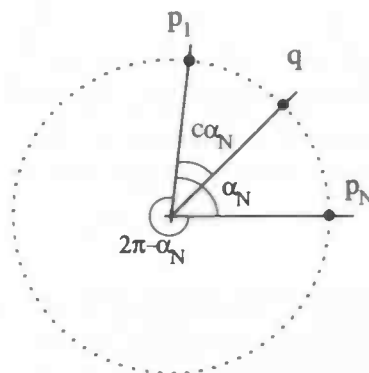


Figure 5.4: Construction of q as a point on the arc of C between p_1 and p_N .

The point q can be described by a constant $c \in [0, 1]$, as shown in Figure 5.4:

$$q = r (\cos(2\pi - c\alpha_N), \sin(2\pi - c\alpha_N))$$

As can be seen in Figure 5.4 and also directly following from the definition of q :

$$\|q - p_i\| = 2r \sin \left(\frac{1}{2} (c\alpha_N + \sum_{k=1}^{i-1} \alpha_k) \right).$$

Inserting this expression for $\|q - p_i\|$ into the equation for $F(q)$ (equation (5.2)) yields

$$F(q) = \frac{1}{2rT} \left[\sum_{i=1}^N \left(\tan \frac{\alpha_i}{4} + \tan \frac{\alpha_{i-1}}{4} \right) 2r \sin \left(\frac{1}{2} (c\alpha_N + \sum_{k=1}^{i-1} \alpha_k) \right) - 4r \right].$$

This can be simplified to

$$F(q) = \frac{1}{2rT} \left[2r \cdot \sum_{i=1}^N \left(\tan \frac{\alpha_i}{4} + \tan \frac{\alpha_{i-1}}{4} \right) \sin \left(\frac{1}{2} (c\alpha_N + \sum_{k=1}^{i-1} \alpha_k) \right) - 4r \right]$$

From Lemma A.3: $F(q) = \frac{1}{T} (g(c) - 2)$. The function value $F(q)$ for any point q on the circle C being negative is then equivalent to $g(c) > 2$, because $T > 0$.

A plot of the function $g(c)$ is shown in Figure 5.5. Because

$$g(c) = \frac{2}{\cos \frac{1}{4} \alpha_N} \cos \frac{1}{4} (1 - 2c) \alpha_N \quad (5.10)$$

is a scaled cosine with $g(0) = g(1) = 2$ for $0 < c < 1$, it can be seen easily that this function is always larger than 2 for any $0 < c < 1$, as long as α_N remains smaller than π : The left factor is always positive for any $0 < \alpha_N < \pi$ and $g(c)$ achieves its maximum at $c = \frac{1}{2}$ and is precisely 2 at $c = 0$ or $c = 1$.

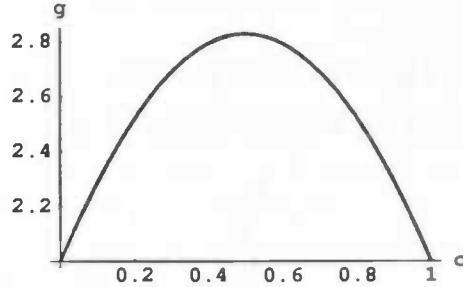


Figure 5.5: Plot of the function $g(c)$ from equation (5.10).

Summary

The function $F(q)$ is positive for every point q on the arc of C between p_1 and p_N . The proof for a similar result on the arcs between the other points p_i, p_{i+1} is a straightforward generalization of the given proof and also follows from the cyclic numbering of the indices.

$F(q) > 0$ for any point $q \neq p_i$ on the circle C and $F(p_i) = 0$ together complete the proof of Theorem 5.6.

5.6 Generalization to convex curves

Throughout the proof of Theorem 5.1 the fact that the curve C is a circle is used only in the determination of the weights. The proof of Theorem 5.1 can be generalized to convex curves:

Let F be the RBF-reconstruction of the vertices of a convex curve C , with one additional constraint p_+ where $F(p_+) = 1$.

$$F(x) = \sum_{i=1}^N w_i \cdot \|x - p_i\| + w_+ \cdot \|x - p_+\| \quad (5.11)$$

Let S be the zero-set $S = F^{-1}(0)$ of this RBF-reconstruction. Then:

THEOREM 5.1

If all the weights w_i are positive and $\sum_{i=1}^N w_i < -w_+$:

1. S is isotopic to C .
2. S preserves the order of the points P on C .

Proof:

Theorem 5.1 can be proven using the same methods for the proof of the circle:

1. Prove that the function F is monotonically decreasing along any line l directed outwards from p_+ .
2. Show that there is a circle C_2 , such that $F(q) < 0$ for any q outside C_2 .

5.6.1 F is monotonically decreasing

Recall from the proof for the circle that the requirement that F is monotonically decreasing along a line l directed outwards of C from p_+ is equivalent to $\langle \nabla F(q), v_+(q) \rangle < 0$. When C is a circle it was shown that each w_i was positive. Assume now, that each w_i is also positive for points as the vertices of a convex polygon C . Then the previous inequality is equivalent to:

$$\sum_{i=1}^N w_i \cdot \langle v_i(q), v_+(q) \rangle_i + w_+ < 0$$

When again writing $\cos \beta_i$ for $\langle v_i(q), v_+(q) \rangle$. This inequality is equivalent to

$$\sum_{i=1}^N w_i \cdot \cos \beta_i + w_+ < 0$$

Because $-1 < \cos \beta_i < 1$ and each w_i is positive this inequality holds when

$$\sum_{i=1}^N w_i < -w_+$$

It can now be concluded that F is monotonically decreasing along any line l directed outwards from p_+ if each $w_i > 0$ and $\sum w_i < -w_+$.

5.6.2 The function becomes negative

Let D be the smallest closed disk centered at p_+ such that all points p_i are within D . Let r be the radius of the disk D . For any point q outside D the distance $\|q - p_i\|$ can be bounded from above as:

$$\|q - p_i\| < \|q - p_+\| + r$$

Let $G(q)$ be defined as

$$G(q) = \sum_{i=1}^N w_i \cdot (\|q - p_+\| + r) + w_+ \cdot \|q - p_+\|$$

Then, for any point q outside D holds: $F(q) < G(q)$. Proving $G(q) < 0$ also proves $F(q) < 0$.

Reducing $G(q)$ yields

$$G(q) = r \cdot \sum_{i=1}^N w_i + \|q - p_+\| \cdot \left(w_+ + \sum_{i=1}^N w_i \right)$$

When assuming all the weights w_i are again positive, this yields the condition

$$\|q - p_+\| > -\frac{\sum w_i}{w_+ + \sum w_i}$$

This yields only a positive distance whenever $\sum w_i < -w_+$

5.6.3 Conclusion

If each weight w_i is positive and $\sum w_i < -w_+$ then the zero-set $S = F^{-1}(0)$ has only one point of intersection with any line l directed outwards from p_+ . The same holds for the convex polygon C (which has P as its vertices).

Each point $q \in S$ is the intersection of a unique line l starting from p_+ . There is also a unique intersection q' of this line l with C . The isotopy can be constructed by linearly interpolating each point $q \in S$ between its corresponding point $q' \in C$. This proves both parts of Theorem 5.1.

There are no restrictions found on the sampling of a convex curve, such that the resulting weights satisfy the conditions.

Chapter 6

Conclusion

During this research project a complete proof has only been found for the correct reconstruction of a circle, as is shown in Chapter 5 under the condition that the angle between two consecutive points (made at the center) is smaller than π .

For the more general situation of convex curves, a proof has been given which includes a general condition on the weights. While a condition on the sampling density was found for a circle, such a condition is still required for a proof for convex curves. This implies that a translation from the condition on the weights must be found to a restriction on the sampling density.

The proof was found for the simple case of a RBF-reconstruction where the polynomial from equation (3.1) was removed and the simple basis function $\varphi(r) = r$ was used. A straightforward extension of the proof to general radial basis functions and with the polynomial included in the implicit function is not possible.

Another open problem is still a proof for surface reconstruction in 3D. Even the simple case of points distributed on a circle is not easily extended to 3 dimensions.

6.1 Future work

The following main directions for future work can be identified.

- For the topological correct reconstruction of a convex curve the condition on the weights should be translated to a condition on the sampling density.
- The prove for points on a circle should be extended to a proof for points on a sphere.
- A method should be found to include the polynomial from equation (3.1) in the proof.
- The main result should be extended to more general basis functions.

Bibliography

- [1] N. Amenta and M. Bern. Surface reconstruction by voronoi filtering. In *Proceedings of the fourteenth annual symposium on Computational geometry*, pages 39–48. ACM Press, 1998.
- [2] N. Amenta, M. Bern, and D. Eppstein. The crust and the β -skeleton: combinatorial curve reconstruction. *Graph. Models Image Process.*, 60(2):125–135, 1998.
- [3] N. Amenta, S. Choi, T. K. Dey, and N. Leekha. A simple algorithm for homeomorphic surface reconstruction. In *Proceedings of the sixteenth annual symposium on Computational geometry*, pages 213–222. ACM Press, 2000.
- [4] J. D. Boissonnat, D. Cohen-Steiner, and G. Vegter. Isotopic implicit surface meshing. In *Proceedings Thirty-Sixth Annual ACM Symposium on Theory of Computing (STOC)*, pages 301–309, Chicago, 2004.
- [5] J. D. Boissonnat and S. Oudot. Provably good surface sampling and approximation. In *Proceedings of the Eurographics/ACM SIGGRAPH symposium on Geometry processing*, pages 9–18. Eurographics Association, 2003.
- [6] T. K. Dey and S. Goswami. Tight cocone: a water-tight surface reconstructor. In *Proceedings of the eighth ACM symposium on Solid modeling and applications*, pages 127–134. ACM Press, 2003.
- [7] T. K. Dey and S. Goswami. Provable surface reconstruction from noisy samples. In *Proceedings of the twentieth annual symposium on Computational geometry*, pages 330–339. ACM Press, 2004.
- [8] M. S. Floater. Analysis of curve reconstruction by meshless parameterization. *Numerical Algorithms*, 32(1):87–98, Jan 2003.
- [9] M. S. Floater. One-to-one piecewise linear mappings over triangulations. *Math. Comput.*, 72(242):685–696, 2003.
- [10] M. S. Floater and M. Reimers. Meshless parameterization and surface reconstruction. *Comput. Aided Geom. Des.*, 18(2):77–92, 2001.
- [11] H. Hoppe, T. DeRose, T. Duchamp, J. McDonald, and W. Stuetzle. Surface reconstruction from unorganized points. In *Proceedings of the 19th annual conference on Computer graphics and interactive techniques*, pages 71–78. ACM Press, 1992.

- [12] W. E. Lorensen and H. E. Cline. Marching cubes: A high resolution 3d surface construction algorithm. In *Proceedings of the 14th annual conference on Computer graphics and interactive techniques*, pages 163–169. ACM Press, 1987.
- [13] S. Plantinga and G. Vegter. Isotopic implicit surface meshing. In *Proceeding Symposium on Geometry Processing, Nice, France, 2004*, pages 251–260, 2004.
- [14] M.J.D. Powell. The theory of radial basis function approximation in 1990. In *W.A. Light (Ed.), Advances in Numerical Analysis Vol. II: Wavelets, Subdivision Algorithms and Radial Basis Functions*, pages 105–210. Oxford University Press, 1992.
- [15] G. Turk and J.F. O'Brien. Variational implicit surfaces. *Technical Report GIT-GVU-99-15, Graphics, Visualization, and Useability Center. Georgia Institute of Technology*, 1999.

Appendix A

Trigonometric Identities

A.1 Weight simplification

LEMMA A.1 (WEIGHT SIMPLIFICATION)

$$\csc 2x - \cot 2x = \tan x.$$

PROOF A.1 (WEIGHT SIMPLIFICATION)

$$\csc 2x - \cot 2x = \frac{1}{\sin 2x} - \frac{\cos 2x}{\sin 2x} = \frac{1 - \cos 2x}{2 \sin x \cos x}.$$

Using $\cos 2x = \cos^2 x - \sin^2 x$ and $\sin^2 x + \cos^2 x = 1$, this can be written as

$$\frac{1 - \cos^2 x + \sin^2 x}{2 \sin x \cos x} = \frac{2 \sin^2 x}{2 \sin x \cos x} = \frac{\sin x}{\cos x} = \tan x.$$

This is the proof of Lemma A.1 \square .

A.2 Tan sin to cos

LEMMA A.2 (TAN SIN TO COS)

$$\tan a (\sin s + \sin(s + 2a)) = \cos s - \cos(s + 2a).$$

PROOF A.2 (TAN SIN TO COS)

$$\tan a (\sin s + \sin(s + 2a))$$

can be written as $(\sin(x + y) = \sin x \cos y + \sin y \cos x)$

$$\tan a (\sin s + \sin s \cos 2a + \cos s \sin 2a).$$

Using $1 + \cos 2x = 1 + \cos^2 x - \sin^2 x = 2 \cos^2 x$ yields

$$\tan a (2 \sin s \cos^2 a + 2 \cos s \sin a \cos a).$$

Because $\tan a = \frac{\sin a}{\cos a}$ one factor $\cos a$ is eliminated

$$2 \sin s \sin a \cos a + 2 \sin^2 a \cos s = 2 \sin a (\cos a \sin s + \cos s \sin a)$$

and this can be combined back into

$$2 \sin a \sin(s + a).$$

Using

$$\begin{aligned} & \cos(x - y) - \cos(x + y) \\ &= \cos x \cos y + \sin x \sin y - \cos x \cos y + \sin x \sin y \\ &= 2 \sin x \sin y \end{aligned}$$

with $x = s + a$ and $y = a$ results in

$$\cos(s) - \cos(s + 2a),$$

completing the proof of Lemma A.2 \square .

A.3 Sum reduction

LEMMA A.3 (SUM REDUCTION)

Consider the function $g(c)$ defined as

$$g(c) = \sum_{j=1}^N \left(\tan \frac{\alpha_j}{4} + \tan \frac{\alpha_{j-1}}{4} \right) \cdot \sin \left(\frac{1}{2} (c\alpha_N + \sum_{k=1}^{j-1} \alpha_k) \right).$$

Then

$$g(c) = \frac{2}{\cos \frac{1}{4} \alpha_N} \cos \frac{1}{4} (1 - 2c) \alpha_N.$$

PROOF A.3 (SUM REDUCTION)

Let

$$\sigma_j = c\alpha_N + \sum_{k=1}^j \alpha_k.$$

Then

$$g(c) = \sum_{j=1}^N \left(\tan \frac{\alpha_j}{4} + \tan \frac{\alpha_{j-1}}{4} \right) \sin \frac{\sigma_{j-1}}{2}.$$

Splitting the sums in two sums results in

$$g(c) = \sum_{j=1}^N \tan \frac{\alpha_j}{4} \sin \frac{\sigma_{j-1}}{2} + \sum_{j=0}^{N-1} \tan \frac{\alpha_j}{4} \sin \frac{\sigma_j}{2},$$

which can be collected back into

$$\sum_{j=1}^{N-1} \tan \frac{\alpha_j}{4} \left(\sin \frac{\sigma_j}{2} + \sin \frac{\sigma_{j-1}}{2} \right) + \tan \frac{\alpha_N}{4} \sin \frac{\sigma_{N-1}}{2} + \tan \frac{\alpha_0}{4} \sin \frac{\sigma_0}{2}.$$

This can be written as

$$\sum_{j=1}^N \tan \frac{\alpha_i}{4} \left(\sin \frac{\sigma_j}{2} + \sin \frac{\sigma_{j-1}}{2} \right) - \tan \frac{\alpha_N}{4} \left(\sin \frac{\sigma_N}{2} + \sin \frac{\sigma_{N-1}}{2} \right) \\ + \tan \frac{\alpha_0}{4} \sin \frac{\sigma_0}{2} + \tan \frac{\alpha_N}{4} \sin \frac{\sigma_{N-1}}{2}.$$

Lemma A.2 will be used to simplify the expression within the leftmost sum. When using Lemma A.2 with $\sigma_j = \sigma_{j-1} + \alpha_k$ and writing out α_0, σ_0 and σ_N ,

$$\sum_{j=1}^N \left(\cos \frac{\sigma_{j-1}}{2} - \cos \frac{\sigma_j}{2} \right) - \tan \frac{\alpha_N}{4} \sin \frac{2\pi + c\alpha_N}{2} + \tan \frac{\alpha_N}{4} \sin \frac{c\alpha_N}{2}$$

can be found. The entire sum can be replaced by $\cos \frac{1}{2}\sigma_0 - \cos \frac{1}{2}\sigma_N$ and because $\sin(\pi + x) = -\sin x$:

$$\cos \frac{\sigma_0}{2} - \cos \frac{\sigma_N}{2} + 2 \tan \frac{\alpha_N}{4} \sin \frac{c\alpha_N}{2}.$$

Again writing out σ_0 and σ_N leaves

$$g(c) = 2 \cos \frac{c\alpha_N}{2} + 2 \tan \frac{\alpha_N}{4} \sin \frac{c\alpha_N}{2},$$

and this can be written as

$$g(c) = \frac{2}{\cos \frac{1}{4}\alpha_N} \cos \frac{1}{4}(1 - 2c)\alpha_N$$

which completes the proof of lemma A.3 \square .

A.4 Proof for the inverse of the distance matrix

To proof the lemma it will be shown that $\Lambda \cdot \Gamma = I$ where I is the identity matrix. Denote the entries of Γ by $\gamma_{i,j}$, $1 \leq i, j \leq N$. It will proven that

$$\sum_{k=1}^N \lambda_{i,k} \gamma_{k,j} = \delta_{i,j},$$

where $\delta_{i,j}$ is the Kronecker delta-symbol. This is performed in two steps:

1. A proof for the entries on the diagonal when $j = i$.
2. A proof for the off-diagonal entries when $j \neq i$.

Diagonal entries of $\Lambda \cdot \Gamma$:

Because $\gamma_{k,i} \neq 0$ only for $k = i - 1, k = i, k = i + 1$

$$\begin{aligned}
 \sum_{k=1}^N \lambda_{i,k} \gamma_{k,i} &= \lambda_{i,i-1} \gamma_{i-1,i} + \lambda_{i,i} \gamma_{i,i} + \lambda_{i,i+1} \gamma_{i+1,i} \\
 &= \gamma_{i-1,i} \sin \sum_{k=i}^{i-2} \beta_k + \gamma_{i,i} \sin \sum_{k=i}^{i-1} \beta_k + \gamma_{i+1,i} \sin \sum_{k=i}^i \beta_k \\
 &= \gamma_{i-1,i} \sin \sum_{k=i-1}^{i-1} \beta_k + \gamma_{i,i} \sin 0 + \gamma_{i+1,i} \sin \sum_{k=i}^i \beta_k \\
 &= \sin \beta_{i-1} \frac{1}{2} \csc \beta_{i-1} + 0 + \sin \beta_i \frac{1}{2} \csc \beta_i \\
 &= \frac{1}{2} + \frac{1}{2} = 1.
 \end{aligned}$$

Off-diagonal entries of $\Lambda \cdot \Gamma$:

Because $\gamma_{k,j} \neq 0$ only for $k = j - 1, k = j, k = j + 1$

$$\begin{aligned}
 \sum_{k=1}^N \lambda_{i,k} \gamma_{k,j} &= \lambda_{i,j-1} \gamma_{j-1,j} + \lambda_{i,j} \gamma_{j,j} + \lambda_{i,j+1} \gamma_{j+1,j} \\
 &= \gamma_{j-1,j} \sin \sum_{k=i}^{j-2} \beta_k + \gamma_{j,j} \sin \sum_{k=i}^{j-1} \beta_k + \gamma_{j+1,j} \sin \sum_{k=i}^j \beta_k.
 \end{aligned}$$

Splitting the sines by using the identities $\sin(a + b) = \sin a \cos b + \cos a \sin b$ and $\sin(a - b) = \sin a \cos b - \cos a \sin b$ gives

$$\begin{aligned}
 \sum_{k=1}^N \lambda_{i,k} \gamma_{k,j} &= \gamma_{j-1,j} \left(\sin \sum_{k=i}^{j-1} \beta_k \cos \beta_{j-1} - \cos \sum_{k=i}^{j-1} \beta_k \sin \beta_{j-1} \right) \\
 &\quad + \gamma_{j,j} \sin \sum_{k=i}^{j-1} \beta_k \\
 &\quad + \gamma_{j+1,j} \left(\sin \sum_{k=i}^{j-1} \beta_k \cos \beta_j + \cos \sum_{k=i}^{j-1} \beta_k \sin \beta_j \right).
 \end{aligned}$$

When writing $\sigma = \sum_{k=i}^{j-1} \beta_k$ and rewriting the result:

$$\begin{aligned}
 \sum_{k=1}^N \lambda_{i,k} \gamma_{k,j} &= (\gamma_{j-1,j} \cos \beta_{j-1} + \gamma_{j+1,j} \cos \beta_j + \gamma_{j,j}) \sin \sigma \\
 &\quad + (-\gamma_{j-1,j} \sin \beta_{j-1} + \gamma_{j+1,j} \sin \beta_j) \cos \sigma.
 \end{aligned}$$

This can be written as a sum of two terms $(\Lambda \cdot \Lambda^{-1})_{i,j} = A \cdot \sin \sigma + B \cdot \cos \sigma$.

Filling in the γ 's in A yields

$$\begin{aligned}
 A &= (\gamma_{j-1,j} \cos \beta_{j-1} + \gamma_{j+1,j} \cos \beta_j + \gamma_{j,j}) \\
 &= \frac{1}{2} (\csc \beta_{j-1} \cos \beta_{j-1} + \csc \beta_j \cos \beta_j - \cot \beta_{j-1} - \cot \beta_j).
 \end{aligned}$$

Because $\csc a \cos a = \cot a$,

$$A = \frac{1}{2} (\cot \beta_{j-1} + \cot \beta_j - \cot \beta_{j-1} - \cot \beta_j) = 0.$$

Filling in the γ 's into B yields

$$\begin{aligned} B &= \gamma_{j+1,j} \sin \beta_j - \gamma_{j-1,j} \sin \beta_{j-1} \\ &= \frac{1}{2} \csc \beta_j \sin \beta_j - \frac{1}{2} \csc \beta_{j-1} \sin \beta_{j-1} \\ &= -\frac{1}{2} + \frac{1}{2} = 0. \end{aligned}$$

This concludes the proof of lemma 5.3 \square .